

# Visualization of Fibrillar Collagen Networks Using Label-Free Nonlinear Optical Microscopy: Deciphering the ECM Structure of 3D-Bioprinted Constructs

S. Shakir<sup>1</sup>, Y.B. Li<sup>2</sup>, C.H. Allen<sup>3</sup>, S. Murugkar<sup>3,4</sup>, L. Mostaço-Guidolin<sup>1,4</sup>

<sup>1</sup>Department of Systems and Computer Engineering, Carleton University, Ottawa, Canada

<sup>2</sup>Human Health Therapeutics Research Centre, National Research Council of Canada, Ottawa, ON, Canada

<sup>3</sup>Department of Physics, Carleton University, Ottawa, Canada

<sup>4</sup>Tissue Engineering and Applied Materials (TEAM) Hub, Ottawa, Canada

**Abstract**— Biological tissues are not exclusively composed of cells. A substantial part of their volume is extracellular space, which is largely filled by an intricate network of macromolecules. Collagens is one of the main components of this complex network, called extracellular matrix (ECM). The ECM serves as the scaffolding for tissues and organs throughout the body, playing an essential role in their structural and functional integrity. Understanding the basic mechanisms involved in the ECM remodelling of tissues provides a window to advance the development of *in vitro* tissue models and enhance tissue engineering applications. In this study, we leveraged one label-free nonlinear optical microscopy imaging modality with a novel microfluidic-based three-dimensional (3D) bio-printing technology to investigate fundamental effects of *in vitro* model design on the cellular ability to remodel fibrillar collagen. Label-free second harmonic generation (SHG) microscopy allowed us to track fibrillar collagen deposition, and our preliminary data indicated that the certain geometries allow cells to remodel ECM more efficiently. Additionally, SHG presents the potential to assess the ECM network development over time, providing important quantitative information crucial to further inform artificial tissues development strategies. Being able to correlate the ECM deposition with cellular behaviour, migration, and even responses to therapeutic treatments, opens a door to enable the biofabrication of complex networks able to mimic a variety of tissue types and pathological conditions.

**Keywords**— ECM, SHG, 3D-Bioprinting, Collagen, Tissue Engineering

## I. INTRODUCTION

Who would think that one day we would be *printing* biological tissues in the same way we transfer ink to paper? Although this sentence oversimplifies a complex process, 3D-bioprinting is one of the most promising technologies of the 21<sup>st</sup> century. 3D models and related “organ-on-a-chip” technologies represent powerful new tools in biomedical research, and 3D-bioprinting has been a major driver of innovation in medicine [1].

Biomaterial and cell combinations, named bio-inks form tissue constructs with pre- designed architecture that enables the creation of complex structures mimicking those naturally found in the human body. Critical factors in 3D bioprinting that influence the final bioprinted construct include selecting the proper bio-ink and bio- materials, identifying the appropriate ratio of cell density, recognizing proper printing geometry and design, and selecting the bioprinting technique

[2]. These factors will impact tissue growth and maturation, and the need for identifying the optimal settings is crucial for achieving desired tissues constructs.

For example, in drug development and fundamental research aimed to understand mechanisms of diseases and repair processes, 3D tissue models capture the complexity of the human tissue microenvironment better than oversimplified cell culture systems. 3D-bioprinted tissue models can more accurately identify and evaluate therapeutic candidates, significantly reducing pre-clinical development costs and accelerating clinical translation [3,4].

A range of 3D functional living tissues may be designed to incorporate diverse spatial heterogeneity of physical properties, cellular composition, and extracellular matrix (ECM) organization, including collagen. Collagen is an important structural component of the ECM, and it forms fibrous networks, which increase the ECM’s structural integrity and facilitates cell adhesion, development, and tissue morphogenesis. Thus, collagen-based hydrogels are frequently used in the tissue engineering field as bio-inks [5].

As the ECM provides physical and chemical cues that regulate cell behavior and orchestrates cellular function in tissue formation and homeostasis, a deeper insight into the effect of the microenvironment on cells can provide invaluable information for disease modeling, understanding its progression, mechanisms and potentially unleash novel treatments.

Visualizing the how collagen fibers are arranged within the ECM network is invaluable to assess the tissue microstructure and further correlate it with cellular behaviours and functions. Nonlinear optical microscopy (NLOM) has been a useful method for observing collagen networks over the past 15 years [6]. Modalities such as the second harmonic generation (SHG) microscopy gained popularity for its ability to image collagen in tissues to a great level of detail and without the need of tissue preparation, staining or any other alteration [7,8]. Combining state-of-art technologies such as 3D-bioprinting and label-free NLO microscopy, this work investigated how the design of bioprinted constructs might influence the capability of cells remodel the ECM, more specifically collagen networks.

## II. METHODS

### A. Cell culture

Commercially obtained Human Fetal Lung (HFL1) fibroblasts cell line was used to remodel the collagen-based bio-ink (CCL-153, ATCC, Manassas, VA, USA) and cultured in Dulbecco's Modified Eagle Medium (DMEM; Invitrogen, Burlington, ON, Canada). The media was supplemented with 1x penicillin-streptomycin and 10% Fetal Calf Serum (FCS) and incubated at 37 °C in humidified 5% CO<sub>2</sub> atmosphere. When cells were confluent, they were harvested with 10% Trypsin-EDTA (Lonza, Bio Whittaker, Walkersville, MD, USA), stained with trypan blue and counted with the Countess<sup>TM</sup> II FL automated cell counter (Invitrogen, Burlington, ON, Canada), to determine the total number of viable cells. Cells were re-suspended in DMEM 10% FCS for experiments.

### B. Bio-ink Preparation

Alginate-based bio-ink (AGC) matrix, 0.75% w/v alginate, MW 186 kDa with PDI 2.1 containing rat tail collagen type I (1.6 mg/ml) was obtained from Aspect Biosystems (Vancouver, Canada). The bio-ink was supplied as a sterile two-part liquid biopolymer, an alginate-containing component (part A) and a collagen-containing component (part B). Prior to printing, AGC matrix part A and part B were kept on ice. Immediately before printing, equal volumes of part A and part B were mixed. The cell density was selected through test prints followed by microscopy evaluation to identify a cell concentration resulting in optimal post-printing viability while allowing acellular gaps to enable cellular attachment and ECM remodelling.

### C. 3D-Bioprinted *in vitro* Models

The *in vitro* models were designed using the Aspect studio software (version 1.3.0.1; Aspect Biosystems, Vancouver, BC, Canada), a 3D Computer-Aided Design (CAD) model of a sheet and ring structures with diagonals and diameters ranging from 6 to 10 mm. The structures had a height of 2 mm. The number of layers was determined by the total structure height divided by the estimated fiber diameter / square diagonal. By assuming a fiber diameter of 100 µm with a 2 mm height design, each construct consisted of 20 ring layers. These ring and sheets structures are adapted from previous studies to maximize cell exposure to media and facilitate oxygen and nutrient access.

### D. Imaging and Image Analysis

The unstained constructs were imaged using a custom-built multiphoton microscope located at the Department of Physics at Carleton University. This microscope utilizes a femtosecond laser (Insight DS+, Spectra Physics, USA), with a wavelength centered at 800 nm and 20 nm bandwidth. Laser power was set to 24 mW at the sample, and output with 120 fs pulses is coupled to an open frame, custom-built laser-scanning microscope. An Olympus UPlanSApo 20X air microscope objective (NA = 0.75 and 0.65 mm working distance) was used in addition to a condenser M Plan APO (Edmund Optics) 20X air (NA = 0.42 and 20 mm working distance). SHG signal was collected in non-descanned mode using a cooled Gallium arsenide (GaAs) photomultiplier tube (H7422-40, Hamamatsu). A 405±20 nm bandpass filter was used in the SHG collection path. ScanImage (Version 5.6, Vidrio Technologies) was used for the control of laser scanning and image acquisition.

Image analysis methods combined with texture analysis allowed us to characterize the fiber organization, fragmentation, thickness, and orientation. Textural features based on image statistics such as first-order statistics (FOS) and gray level co-occurrence matrix (GLCM) parameters were extracted from the SHG images all constructs. Different collagen accumulation patterns in rings and sheet-shaped constructs can be successfully tracked using these image statistics, thus providing a solid foundation for assessment of ECM remodelling. Specific fiber orientation properties were obtained by evaluating the gradient structure tensor in a local neighbourhood, based on the ImageJ OrientationJ plugin. The plugin computes the orientation, energy and coherency maps of an image and its weighted orientation histogram, and outputs a Hue-Saturation-Brightness (HSB) color-coded map which shows the angles of the oriented structures in the image.

## III. RESULTS

### A. Texture Analysis of Collagen Networks at Different Regions of 3D-Bioprinted Constructs

Five textural parameters were extract from all SHG images: energy, contrast, correlation, entropy, and inverse difference moment (IDM). This section investigates the assumption that ring-designed structures can tolerate a higher cell proliferation rate, as well as allow for cells to synthesize more organized collagen networks compared to the sheet structure. It was hypothesized that the sheet structure is limited in allowing nutrients to diffuse and for oxygen transport to the middle of the structure, both of which affect

cellular migration, communication, and ability to remodel the ECM. On the other hand, the ring structure can constrain cells to a specific geometry that allows easier access to oxygen and nutrients. In Fig. 1A we have representative SHG images of areas of interest in both constructs, being those the edge of the ring structures (ER) and edge of the sheets (ES), and well as the centres of each one, defined here as middle of the ring (MR) and middle of sheet (MS) structures.

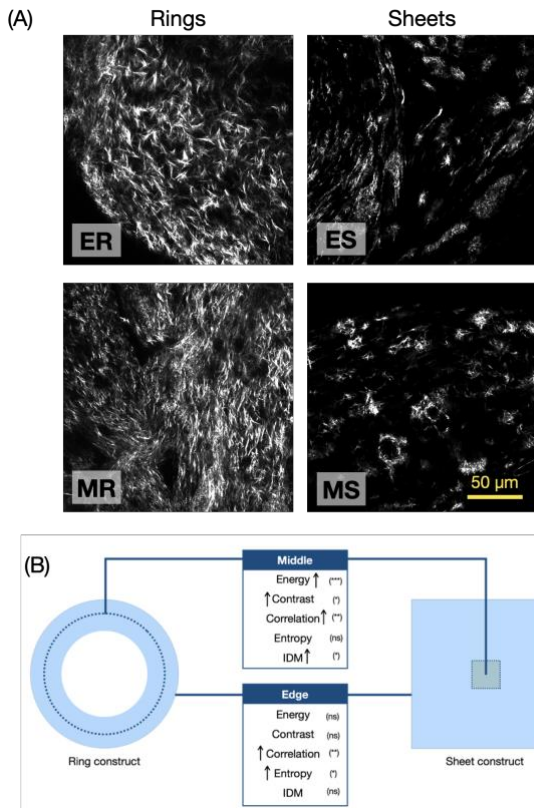


Fig. 1 (A) Representative SHG images of fibrillar collagen networks found on 3D-bioprinted constructs. Different geometries facilitate ECM remodelling and (B) texture analysis of such images allows to quantify morphological changes of the tissue structure. ER: edge of rings; ES: edge of sheets; MR: middle of rings; MS: middle of sheets. IDM: inverse difference moment.

Based on textural features, it was found that energy, representing the orderliness of the collagen network, was not significantly different between the edges of each construct. However, when comparing the ER to the MR, ER had a higher energy value, similarly with the MS compared to the MR. There was no significant difference in contrast for both regions in the sheet constructs, but the MR had a higher contrast value than the ER. There was no statistical difference found between the ER and the ES, but the contrast of the MR

was higher than the contrast of the MS. As mentioned previously, a higher contrast is often an indicator of collagen fibers not having a preferred orientation due to the formation of bundles.

Correlation, on the other hand, presented significant differences in both regions of both constructs. A high correlation value suggested that there is a high probability of one or more patterns repeating themselves inside the computational window, suggesting different levels of collagen remodelling happening on each construct, facilitated by its geometry. Entropy was another textural feature indicating the remodelling difference.

Finally, ES and ER presented a similar density of collagen, but when comparing MR to the MS, a significant difference was observed. This difference was accounted for by calculating IDM, where a higher value can be associated with a denser collagen fibrillar structure. A schematic summary of all textural parameters associated to the structure of fibrillar collagen accumulated on different regions of the constructs is presented in Fig.1B.

### B. Fiber Orientation and Remodelling Over Time

Texture analysis allowed us to quantify the organization levels of the collagen deposited to form the ECM of the engineered tissues. Sheet structure presented a less organized collagen morphology, and here we present preliminary results associated to the capability of using SHG images to assess the orientation of collagen fibers at different regions of the constructs and time points.

There is a statistical difference between the ER and MR in collagen orientation. The central region of the ring constructs (MR) presented collagen fibers that were well organized in the 60 to 90 degrees, and -60 to -90 degrees, while the edge presented more fibers organized at the 0 degrees as well. In addition to tracking these differences within each construct, SHG images also allowed us to track time-dependent changes in collagen fibrillar morphology. Tests were conducted on the ring-shaped 3D-bioprinted construct.

While contrast textural feature provides us with some insights into orientation, further analysis allows us to identify preferred directions of the fibers and arrangements. Fig.2 shows the collagen fibers orientation distribution on each day (observed over a period of 10 days) and representative colour maps, and the angular distribution of fibers and fiber fragments. There were no statistical differences observed between day 1 and day 4. However, after day 4, the collagen network became less organized with more fibers being oriented at different angle. This pattern continued until day 10, where this collagen network disorganization was still observed.

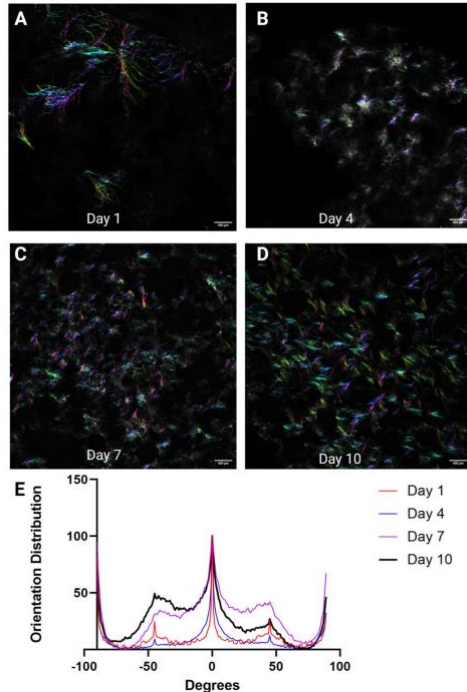


Fig. 2 (A-D) Representative SHG images of fibrillar collagen networks imaged at different time points, from 3D bioprinted constructs (ring-shaped geometry). (E) The fibrillar collagen orientation changes significantly between 4 to 7 days period, indicating ECM remodelling.

Although further studies are needed to gather additional evidence to support these results from the cellular biology perspective, these observations provide evidence of how label-free imaging technologies are crucial to track changes on engineered tissues, such as the effect of design or a more accurate definition of relevant time points linked to specific cellular activities.

#### IV. CONCLUSIONS

With the concept of tissue engineering, 3D bioprinting of biological tissues has been of emerging interest due to its promise to generate *in vitro* models and organ-like constructs that can be used towards understanding fundamental; disease mechanisms, its progression, or as testing bed for novel therapies. Investigating these models and how different 3D bioprinting designs influence the cellular responses, migration, communication, and the overall potential of having structures which resemble tissues, may be a step towards 3D bioprinted functional organs.

This preliminary study shows that the 3D bioprinted design choice has a major effect on cellular activity and collagen deposition behaviour. These findings were made possible thanks to the integration of state-of-the-art imaging

strategies and specific image analysis methods, aimed to capture the unique fiber-like structure of the synthesized ECM. While these findings indicate that the image analysis techniques presented and used in this research can further provide information necessary to optimize bioprinting parameters, using other imaging modalities and strategies can enhance our understanding of the changes happening within cellular microenvironment and how they might be associated to cellular behaviour.

#### ACKNOWLEDGMENT

This work was supported by the Natural Sciences and Engineering Research Council (Discovery Grant of Canada, RGPIN-2021-04185), National Research Council, Ideation Programs – New Beginnings Fund and Carleton University (Research Development Grant 2020/21).

#### CONFLICT OF INTEREST

The authors declare that they have no conflict of interest.

#### REFERENCES

1. W. Jamroz, J. Szafraniec, M. Kurek, and R. Jachowicz, "3D printing in pharmaceutical and medical applications—recent achievements and challenges", *Pharmaceutical research*, 35, pp.1-22, 2018. DOI: 10.1007/s11095-018-2454-x
2. K. A. Deo, A.S. Kanwar, W. P. Charles, Alge D.L., and Gaharwar A.K., "Bioprinting 101: design, fabrication, and evaluation of cell-laden 3D bioprinted scaffolds." *Tissue Engineering Part A* 26, no. 5-6 pp. 318-338, 2020. DOI: 10.1089/ten.tea.2019.0298
3. W. Peng, U. Derya, and I.T. Ozbolat, "Bioprinting towards physiologically relevant tissue models for pharmaceuticals." *Trends in biotechnology* 34,9pp.722-732,2016.DOI: 10.1016/j.titech.2016.05.013
4. E. Niederberger, Parnham M.J., Maas J., and Geisslinger G.. "4 Ds in health research—working together toward rapid precision medicine." *EMBO Molecular Medicine* 11, no. 11, e10917, 2019. DOI: 10.15252/emmm.201910917
5. E. O. Osidak, Kozhukhov V.I., Osidak M.S., and Domogatsky S.P. "Collagen as bioink for bioprinting: A comprehensive review." *International journal of bioprinting* 6,3,2020. DOI: 10.18063/ijb.v6i3.270
6. W. R. Zipfel, Williams R.M., and Webb W.W. "Nonlinear magic: multiphoton microscopy in the biosciences." *Nature biotechnology* 21.11, pp.1369-1377, 2003. DOI:10.1038/nbt899
7. L.B. Mostaço-Guidolin, Rosin N.L., and Hackett T.L. "Imaging collagen in scar tissue: developments in second harmonic generation microscopy for biomedical applications." *International journal of molecular sciences* 18, 8, pp.1772, 2017. DOI: 10.3390/ijms18081772
8. P.J. Campagnola, Loew L.M. "Second-harmonic imaging microscopy for visualizing biomolecular arrays in cells, tissues and organisms." *Nat. Biotech* 21.11,pp.1356-1360,2003. DOI:10.1038/nbt894
9. G. Addario, Djudjaj S., Fare S., Boor P., Moroni L., and Mota C. "Microfluidic bioprinting towards a renal *in vitro*